

3.0 Dielectric Properties Measurement Methodology

3.1 Available Methods

The dielectric properties of materials have been shown to be very dependent on the frequency of their measurement. No one measurement technique is available, however, that will give the entire frequency range needed to characterize the entire spectrum. Several techniques are therefore used, each useful only in a certain frequency range [15]. A summary of these methods are shown in Table 2.

Table 2: Experimental Methods for the Measurement of Dielectric Properties [15]

Frequency Range (Hz)	Method
10^{-4} to 10^{-1}	D.C. Transient Measurements
10^{-2} to 10^2	Ultra Low Frequency Bridge
10 to 10^7	Schering Bridge and Auto Balancing Bridge
10^5 to 10^8	Resonance Circuits
10^8 to 10^9	Coaxial Line and Re-entrant Cavity
10^9 to 3×10^{10}	H_{01n} Cavity Resonator and Waveguides

The methods shown in Table 2 can generally be divided into two groups. Those less than 10^8 Hz are referred to as lumped circuit methods, while those greater than 10^8 Hz are called distributed circuit methods. The lumped circuit methods are designed to measure a cell capacitance and resistance which can be related to the dielectric properties of the sample. In contrast distributed circuits are designed to measure an attenuation factor, α , and a phase factor, β , which may also be related to dielectric properties.

3.2 Dielectric Property Measurement Principle

It has been shown in the previous section that the dielectric properties of a material

can be measured many ways. However often the nature of the materials to be measured, the application, the desired precision and the equipment costs severely limit the experimental approaches. For the current research an experimental set-up was required that could non-invasively measure the dielectric properties of both solid and liquid materials in-situ. The application for use as an on-line sensor dictated that the approach be relatively inexpensive. As a result a set-up was devised in which a parallel plate capacitor was arranged as the key component of a LRC network. Using a HP-4194A Impedance/Gain Phase Analyzer, the frequency dependent capacitance and resistance of the capacitor containing the desired sample could be monitored and related to the dielectric properties of the sample. The HP-4194A was chosen because of its wide frequency range(100 Hz-40 MHz) and low cost(relative to analyzers in the microwave region). The use of the parallel plate capacitor allows for easy on-line measurement since the capacitor can be placed directly into a dip-pan containing a ceramic slurry or with the electrodes on each side of an infiltrated fiber mat(see Fig. 2).

The dielectric properties of the materials in this study were therefore measured with a HP-4194A Impedance/Gain-Phase Analyzer in concert with a self-designed test cell that incorporated a parallel plate capacitor. The dielectric sample placed in the capacitor can be considered electrically equivalent to a capacitance, C_x , in parallel with a resistance, R_x , Fig. 16, where C_x represents the samples ability to store charge and R_x represents its heat related loss[17].

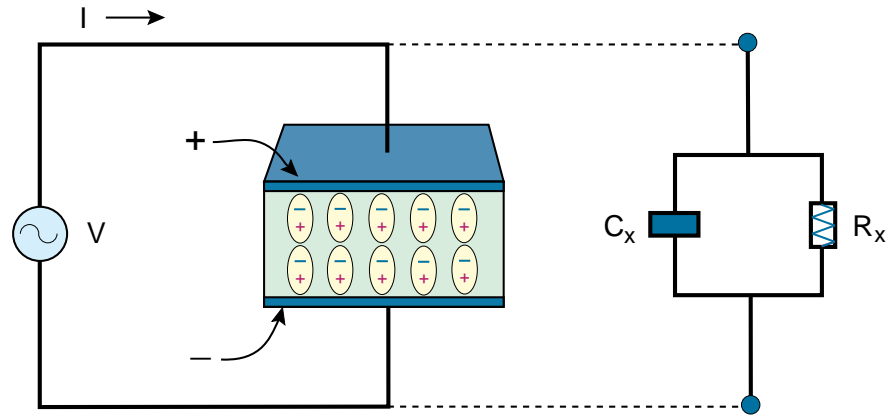


Figure 14. A Parallel plate capacitor containing a dielectric material and it equivalent circuit[17]

These values, C_x and R_x , could be measured using the impedance analyzer(see section 3.4) and related to the dielectric properties of the sample as

$$\epsilon' = \frac{C_x}{C_o} \quad (38)$$

$$\epsilon'' = \frac{1}{R_x \omega C_o} \quad (39)$$

$$\tan \delta = \frac{1}{R_x C_x \omega} \quad (40)$$

where C_o is the cell capacitance in vacuum and is related to the electrode spacing and the electrode area through

$$C_o = \frac{A \epsilon_o}{d} \quad (41)$$

where A is the electrode area, d is the electrode spacing, and ϵ_o is the permittivity in vacuum given as 8.854×10^{-12} pF/m[15].

3.3 Test Cells

The research conducted required the measurement of both liquid and solid materials, with the ability to simultaneously measure the weight and the dielectric constant of the solid sample for tape drying experiments. Two separate test cells were found to be required. To prevent erroneous results caused by fringing effects, Fig. 15, each cell used a three-terminal arrangement[45] in which a guard electrode was used to prevent the unwanted fringing effects, Fig. 16.

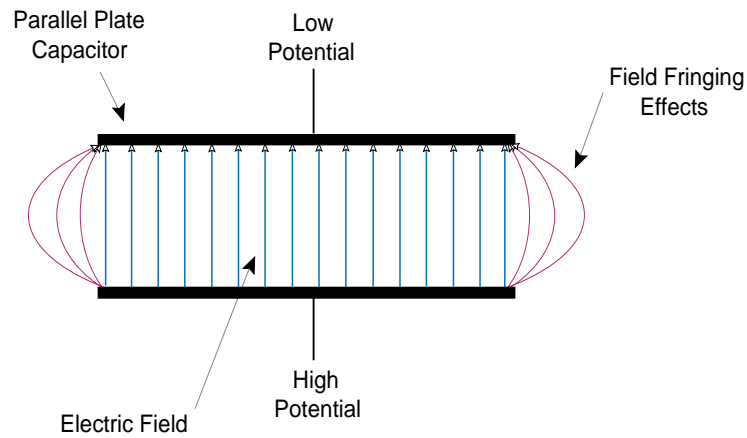


Figure 15. A schematic representation of electric fringing effect of an unguarded parallel plate capacitor

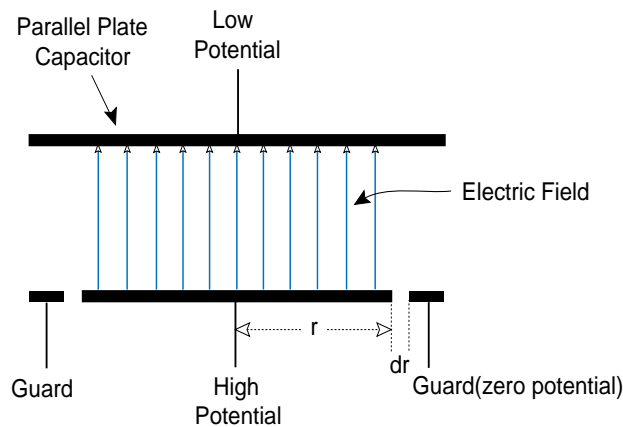


Figure 16. Three-terminal electrode arrangement[15]

Using this arrangement an effective electrode area, A_e , must be used in equation (41). The effective area accounts for the gap between the low electrode and the guard ring and can be expressed as

$$A_e = \pi \left(r + \frac{dr}{2} \right)^2 \quad (42)$$

3.3.1 Liquid Cell

The measurement of the dielectric properties of a tape casting slurry required a test cell that was resistant to the corrosive nature of the slurries, contained adjustable electrode spacing to account for the possibility of the necessity to measure solid samples of varying thickness or liquid samples using different electrode spacings which may present themselves in sensing applications, and was desired to be comprised of materials that were easily machinable.

The resulting cell, Fig. 15, consisted of a polyethylene container that was designed to hold a liquid sample and remain chemically resistant to the solvents used in tape casting. Inside the container two copper electrodes and a copper guard ring were arranged in the three-lead set up. Copper was chosen due to its machinability and excellent conductivity. The guard ring and the low electrode were 1.5" in diameter and the high electrode was 1.0" in diameter. The spacing of the electrodes was controlled by a micrometer and the electrodes were aligned using two chemically resistant teflon guides. The cell temperature was monitored using a resistance temperature device (RTD).

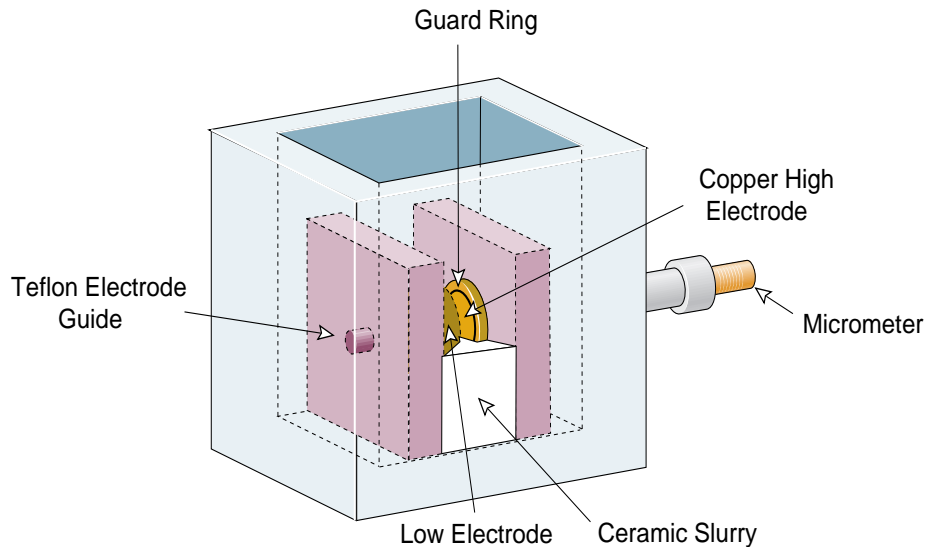


Figure 17. Schematic drawing of the liquid test cell

3.3.2 Drying Test Cell

The drying test cell required that the dielectric constant of a solid sample be determined while simultaneously measuring the weight. In addition, the electrode spacing needed to be adjustable so that an ideal electrode spacing could be determined that allowed for accurate dielectric measurement while maintaining the balance of the scale during measurement. A permeable electrode was desired to alleviate the condensation of liquid onto the electrode surface during evaporation. Such an effect was observed during initial measurements using solid electrodes.

To satisfy the above requirements this test cell, Fig. 18, used a non-contacting electrode method to measure the dielectric constant of the sample. For such a method, equation (3) is replaced by[46]:

$$\epsilon' = \frac{1}{1 - \left(1 - \frac{C_1}{C_2}\right) \times \frac{t_g}{t_a}} \quad (43)$$

where C_1 and C_2 are the measured capacitances without and with the sample present respectively and t_g and t_a are the gap between the two electrodes and the sample thickness respectively.

This cell consisted of two platinum plated niobium mesh electrodes, to help alleviate the condensation problem, which were mounted on polyethylene supports. The low electrode was surrounded by a stainless steel guard electrode and also mounted on a polyethylene support. The electrode spacing was again controlled by a micrometer. The drying sample was mounted on a thin(0.006”) glass slide and mounted onto a sample holder. The holder was set on a precision scale. This set-up enabled the simultaneous measurement of the sample capacitance and weight so the variation of capacitance with solvent removal could be monitored. Temperature was controlled by placing the cell in a oven.

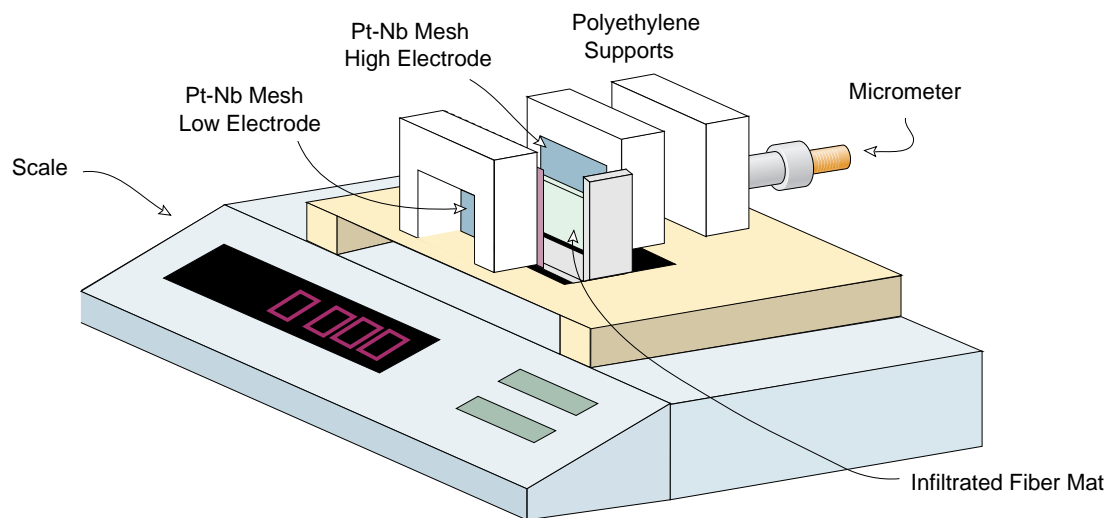


Figure 18. Schematic representation of the drying test cell

3.4 Dielectric Measurements Using a Network Analyzer

The complete experimental set-up, Fig. 19, consisted of the designed test cells attached to a HP-4194A Impedance/Gain-Phase Analyzer using coaxial wires and a HP-16047C test fixture. The high potential and low potential electrodes were connected to the HP-16047C test fixture which in turn interfaced with the analyzer, Fig. 20, where H_p is the high potential, H_c is the high current, L_p is the low potential and L_c is the low current. The guard electrode was connected to ground. A personal computer was used for data acquisition.

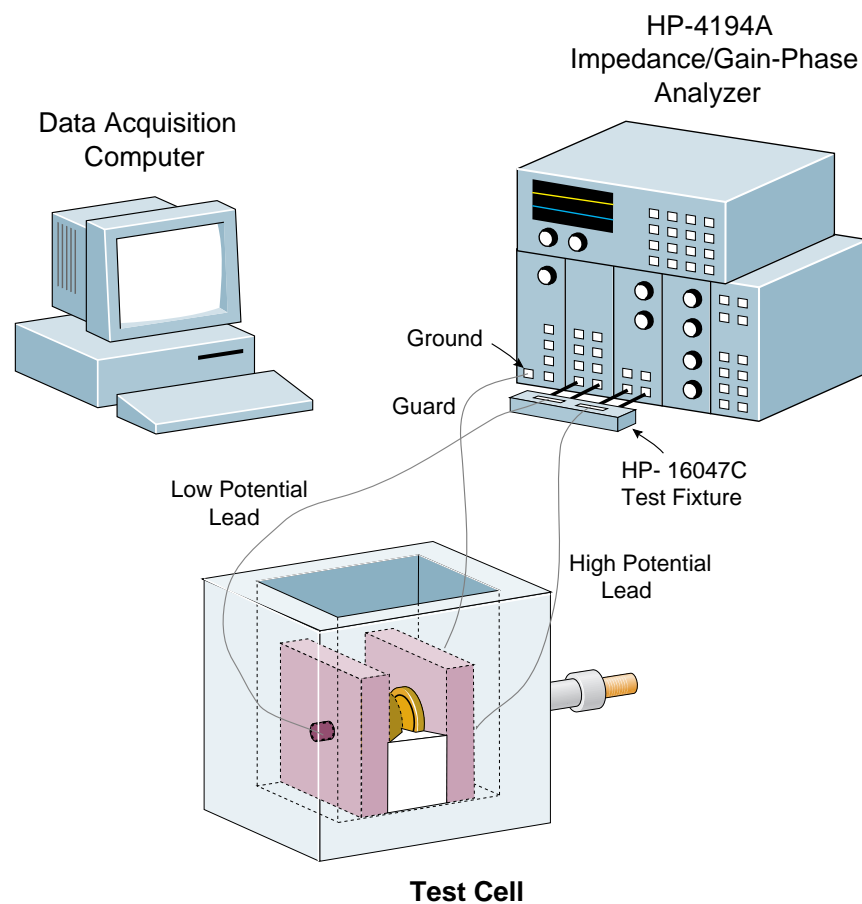


Figure 19. A schematic diagram of the experimental set-up consisting of a HP-4194A Impedance/Gain-Phase analyzer, a test cell, and a data acquisition computer

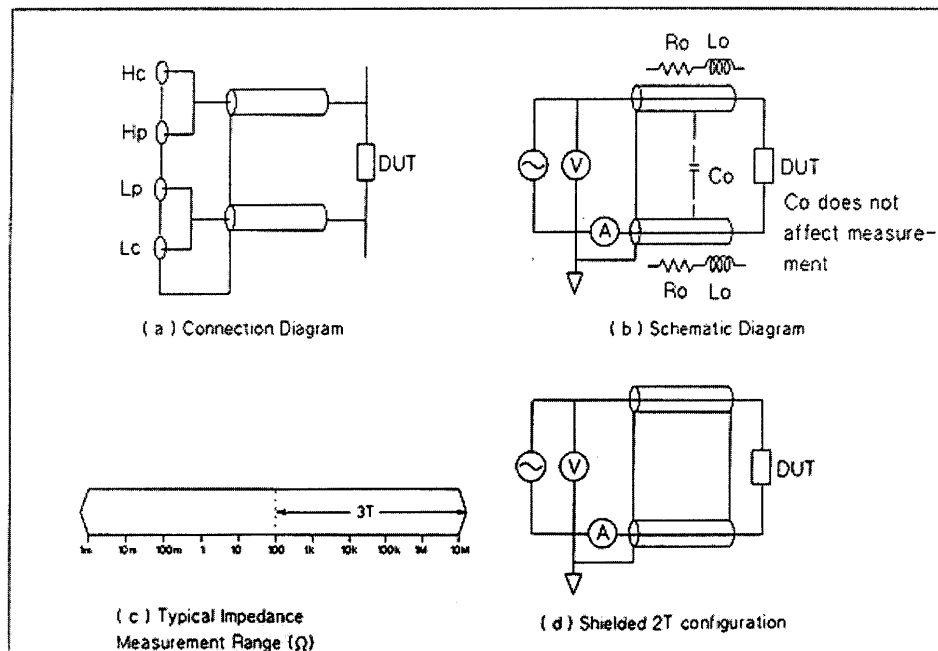


Figure 20. A schematic diagram showing the test cell/analyzer interface using a HP-16047C test fixture

The analyzer uses an auto balancing bridge method[47] to measure to the impedance of a equivalent circuit, Fig. 21.

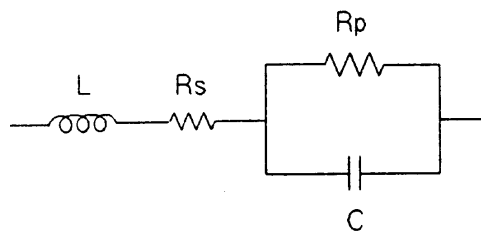


Figure 21. Equivalent circuit for a capacitor connected to a HP-4194A Impedance/Gain-Phase analyzer[47]

The impedance, Z , is complex and given as

$$Z = R + jX = R_s + \frac{R_x}{1 + \omega^2 R_x^2 C_x^2} + j \frac{\omega L - \omega^2 R_x C_x + \omega^3 R_x L C_x}{1 + \omega^2 R_x^2 C_x^2} \quad (44)$$

where R is the resistance and X is the reactance. Using this measurement the capacitance of the capacitor is calculated using the relationship[47]

$$C = \frac{1}{\omega X} \quad (45)$$

where ω is the test frequency. In addition the cell conductance, G, could also be calculated by

$$G = \frac{1}{R} \quad (46)$$

The values of R_s and L(inductance) are parasitic values in the equivalent circuit due to the lead wires and the electrodes while C_x and R_x can be related to the charge storage and loss in the of the dielectric material in the capacitor respectively(see Fig.14 and equations (38) and (39)). To limit the parasitic effect the leads were kept as short as possible and shielded. As the measurement frequency is increased, however, the effect of L also increased and its existence was seen as a resonance point in the calculated circuit parameters. This inductance resonance effectively limited the measurement of the dielectric properties to 1 MHz[47].

The accuracy of the analyzer could be controlled to some extent by several measurement parameters. These parameters include the test frequency(due to the inductance effect), the number of measurements averaged, the intergration time of the measurement, and the applied voltage to the cell[48]. How these parameters affected the accuracy of the

cell is presented in the following section.

3.5 Experimental Error

The error in the measurement of dielectric properties using the test set-up described in the previous section could be attributed to the intrinsic precision of the equivalent circuit parameter measurement using the analyzer and unknown differences between the “sensed” and sample temperature. The effect of each was estimated and is presented below.

3.5.1 Intrinsic precision of the HP-4194A analyzer

The measurement of the capacitance and the resistance with a HP-4194A analyzer has errors associated with the test frequency range, the number of measurements averaged, the integration time of the measurement, and the applied voltage to the cell. These errors can be determined using the HP-4194A manual[48]. The accuracy of the capacitance calculated was determined using the following relationship

$$C_a = \frac{A_1}{\alpha} + A_2 + \left(\frac{B_1}{|Z_c|} + B_2 \times |Z_c| \right) \times \frac{100}{\alpha} \quad (47)$$

where

$$|Z_c| = \frac{1}{2\pi\omega C_m} \quad (48)$$

C_a is the percent error in the capacitance measurement, C_m is the capacitance value calculated from the impedance measurement, α is the test signal level in volts(0.5) and A_1 , A_2 , B_1 and B_2 are values determined using the graph in Fig.22. These values depend on the

The capacitance and resistance measurements are related to the dielectric properties using equations (38)-(41). As a result, the uncertainty in ϵ' is dependent on C_a , the uncertainty in ϵ'' is dependent on R_a and the uncertainty of $\tan(\delta)$ on both values. The intrinsic error in C_o was accounted for with a cell calibration(see section 3.6).

3.5.2 Measurement error due to temperature deviation

The error in the temperature measurement of the liquid test cell(Fig. 17) was found to be 1.6%. This error was determined by repeated measurement of ethanol at 25.0°C. This deviation can be attributed to temperature inhomogeneity or a temperature gradient in the sample along with a variation in thermocouple position. These measurements were performed in the liquid test cell.

3.6 Cell Calibration

The designed test cells were calibrated using materials with known dielectric properties. The liquid test cell was calibrated using ethanol and the drying test-cell was calibrated using a teflon sample. Using this approach the parasitic effects in the leads and minor electrode misalignment were taken into account. Several other known materials were then measured to verify the results. These results are shown in Table 3 and Table 4.

Table 3: Dielectric Constant of Known Materials Using Liquid Test Cell(@ 1MHz)[49]

Solvent	ϵ' (Handbook)	ϵ' (Measured)
Acetone	20.5	20.91
Isopropyl Alcohol	20.0	19.9
Methanol	32.4	32.93
Ethanol	24.5	24.5

Table 4: Dielectric Constant of Known Materials Using Non-Contacting Test Cell(@ 1MHz)[49]

Material	ϵ' (Handbook)	ϵ' (Measured)
Teflon	2.21	2.21
Polyethylene	2.25	2.31
Silicone Rubber	6.00	6.12
Nylon 66	3.65	3.75

The error in the liquid test cell observed in the calibration experiments(1.6%) appear to be the same order of magnitude as the observed reproducibility error in the liquid test cell(~2.0%). With inaccuracy in the temperature measurement being the largest source of error. The drying test cell had a slightly higher error(~3.0%) than the liquid test cell which can be attributed to the increased difficulty in accurately controlling temperature using this test cell.

3.7 Additional Sources of Uncertainty- Electrode Polarization

In addition to the intrinsic error in the analyzer and the systematic error in temperature measurement, erroneous readings can also arise due to the existence of an interface

between the sample and the electrodes resulting in electrode polarization. This effect is essentially a interfacial polarization effect(see section 2.5) due to the conductivity differences between the sample and the electrodes. This effect becomes increasingly important as the frequency is decreased and as the conductivity of the sample is increased. Several methods have been proposed to account for this error[33,50,51,52]. A method by Fricke and Curtis[33] accounts for the effect by the measurement of the dielectric constant at two electrode spacings. This allowed for the dielectric constant of a sample to be determined without knowing the magnitude of the interfacial polarization at the electrodes. In addition Oncley[52] and Johnson and Cole[51] have presented empirical relationships. Oncley's relationship is given as

$$\epsilon = \left(C - C_o - AG\omega^{-\frac{3}{2}} \right) \frac{d}{K} \quad (50)$$

where C is the measured cell capacitance for an electrode spacing d, and C_o and K are constants of the cell. The term AG $\omega^{-3/2}$ takes into account the electrode polarization effect where A is the slope of a plot of (C-C_o) vs. G² $\omega^{-1/2}$ in a region removed from the electrode polarization effect, G is the cell conductance, and ω is frequency. Results have shown[53] that the relationship is only valid for frequencies greater than 25 kHz. Johnson and Cole's relationship is given as

$$\epsilon_m = \epsilon' + \left(Z_o \sin \frac{n\pi}{2} \right) \omega^{-(n+1)} \left(\frac{G^2}{C_o} \right) \quad (51)$$

where ϵ_m is the measured dielectric constant and Z_o and n are constants of the test cell.

This relationship was found to be useful to frequencies as low as 20 Hz in a formic acid sample.